Supporting Information

Molecular brush: an ion-redistributor to homogenize fast Zn^{2+} flux and deposition for calendar-life Zn batteries†

Huanyan Liu[a], Qian Ye[a], Da Lei[a], Zhidong Hou[a], Wei Hua[a], Yu Huyan[a], Na Li[a], Chunguang Wei[b], Feiyu Kang[c], Jian-Gan Wang[a,*]

[a] State Key Laboratory of Solidification Processing, Center for Nano Energy Materials, School of Materials Science and Engineering, Northwestern Polytechnical University and Shaanxi Joint Lab of Graphene (NPU), Xi'an 710072, China

[b] Shenzhen Cubic-Science Co., Ltd, Nanshan District, Shenzhen 518052, China

[c] Engineering Laboratory for Functionalized Carbon Materials and Shenzhen Key Laboratory for Graphene-based Materials, Graduate School at Shenzhen, Tsinghua University, Shenzhen

*Corresponding author.E-mail: wangjiangan@nwpu.edu.cn

† Electronic supplementary information (ESI) available.

Experimental Section

Synthesis of PSPMA coated Zn anode (PSPMA@Zn): For the synthesis of PDA@Zn, dopamine (0.2 mg mL^{-1}) was dissolved in 10 mM Tris-HCl (pH 8.5), and Zn anodes were dipped into the solution. The PDA@Zn was obtained after standing for a certain time in air. For the synthesis of PSPMA@Zn electrodes, firstly, 2 g of anionic 3-sulfopropyl methacrylate potassium salt (SPMA) monomer was dissolved in 10 mL of H_2O/MeOH (2: 1) solution. Then, the PDA@Zn anodes were immerged in the solution and degassed by N_2 to remove the dissolved O_2. Afterwards, the sealed vessel was placed under a UV equipment (300 W) for 1 h, 10 cm away from the light source. The PSPMA@Zn was obtained after being alternatively washed with DI water and ethanol.

Synthesis of MnO_2: Typically, 4 mM $KMnO_4$ was dissolved in 100 mL deionized (DI) water. After 10 min of magnetic stirring, 6 mM zinc powder was added to the solution and mixed well. The reaction occurs when 10 mL of 2 M H_2SO_4 was added dropwise to the above mixture. After continuous magnetic stirring at room temperature for 2 h, the resulting black precipitate was washed alternately with DI water and ethanol for several times. Finally, MnO_2 powder was obtained after drying in an oven at 60 °C for 12 h.

Assembly of Zn//Cu asymmetric cells, Zn//Zn symmetric cells, and Zn//MnO_2 full cells: In this work, CR2025-type coin cells were used as the assembling model. For the preparation of MnO_2 cathode, MnO_2 powder, polyvinylidene fluoride (PVDF), and conductive carbon black were mixed in a weight ratio of 7:2:1 with N-methyl-2-

pyrrolidone (NMP) as the solvent. The MnO_2 electrode was obtained after casting the slurry onto a titanium foil and drying at 60°C for 24h under vacuum. The mass loading of MnO_2 was about 1.2 mg cm^{-2} in one cell. All the electrodes, involving Cu, Zn, and MnO_2, were tailed to a diameter of 12 mm. For the assemble of Zn//Cu and Zn//Zn cells, the two electrodes were sandwiched by a piece of glass fiber separator (GF/D type) filling with 2 M $ZnSO_4$ electrolyte. Zn//MnO_2 full cells were assembled by using bare Zn or PSPMA@Zn as anode, 2 M $ZnSO_4$ + 0.1 M $MnSO_4$ as electrolyte, and glass fiber as separators. All batteries were assembled in open air and aged for 12 hours before electrochemical tests. Mn^{2+}-salt was added into electrolyte to ensure the structural stability of MnO_2 cathode by suppressing the disproportionation reaction.

Preparation of PAM electrolyte: 1 g of acrylamide monomer powders was added into 10 g of DI water and stirred for 30 min at 25 °C to fully dissolve. Then, 5 mg of potassium persulfate (initiator) and 2 mg of N,N′-methylenebis(acrylamide) (cross-linker) were added into the above solution and stirred for 1 h at 25 °C. After the solution was degassed in a vacuum chamber, the mixed solution was poured into a mold and kept at 50°C for 4 h to obtain the PAM hydrogel. Finally, the PAM hydrogel was soaked in 50 mL of mixed solution of 2 M $ZnSO_4$ and 0.1 M $MnSO_4$ up to 12 h to achieve the equilibrated state.

Materials characterization: The physical morphologies of the electrodes were investigated by field-emission scanning electron microscopy (SEM, NanoSEM 450, FEI). The element and surface chemistry of the interlayer was analyzed by X-ray photoelectron spectroscopy (XPS, ESCALAB 250Xi, Thermo Scientific). Attenuated

total reflection infrared (ATR-IR) spectroscopy was performed on a ThermoNicolet iS50 FTIR spectrometer. Atomic force microscopy (AFM) was carried out on a Bruker Dimension Icon microscope in a tapping mode. The crystallographic structure of the samples was studied by X-ray diffractometer (XRD, X'Pert PRO MPD, Philips) using Cu-Kα as the radiation source (λ= 1.5418 Å). The contact angle measurements were recorded on an OCA25 measuring system (Dataphysics, Germany) to evaluate the surface wettability of the electrodes.

Electrochemical measurement: All the rate and cycling performance of the assembled cells were tested on the Neware Battery Testing System at room temperature. Electrochemical impedance spectra (EIS), cyclic voltammetry (CV) curves, Zn^{2+} transference number (t_{Zn2+}), and Chronoamperometry (CA) measurement were collected on the Solartron electrochemical workstation (1400 + 1470E, England). Specifically, EIS plots were measured at frequencies of 100 kHz to 10 mHz with a perturbation amplitude of 5 mV, while CV curves of the full cells were tested at a scan rate of 0.1 mV s^{-1}.

Computational details: First-principles calculations were performed using the generalized gradient approximation (GGA) and the Perdew-Burke-Ernzerhof (PBE) exchange-correlation function in the DMol3 module of Materials Studio. An all-electron numerical basis set (DNP basis set) with polarization functions using the DFT-D method in the Grimme scheme. Convergence tolerances were set to energy 1.0×10^{-5} Ha (1 Ha = 27.21 eV), maximum force of 2.0×10^{-3} Ha $Å^{-1}$, and maximum displacement of 5.0×10^{-3} Å. The simulation of Zn matrix with Zn atom was taken

using a five-layer 2 × 2 supercell with top three-layer atoms releasable. The initial position of the Zn atom was set at the apex of the tetrahedron by the closest packing. SPMA molecule was used to simulate the adsorption behavior with Zn atom or H_2O molecule. The binding energy (E_b) can be calculated by the following equation:

$$E_b = E_{total} – E_{sub} – E_{ads}$$

E_{total} and E_{sub} represent the total energy of the adsorbed model and the energy of metal or SPMA substrate, respectively, while E_{ads} represents the energy of the adsorbed Zn atom or H_2O molecule.

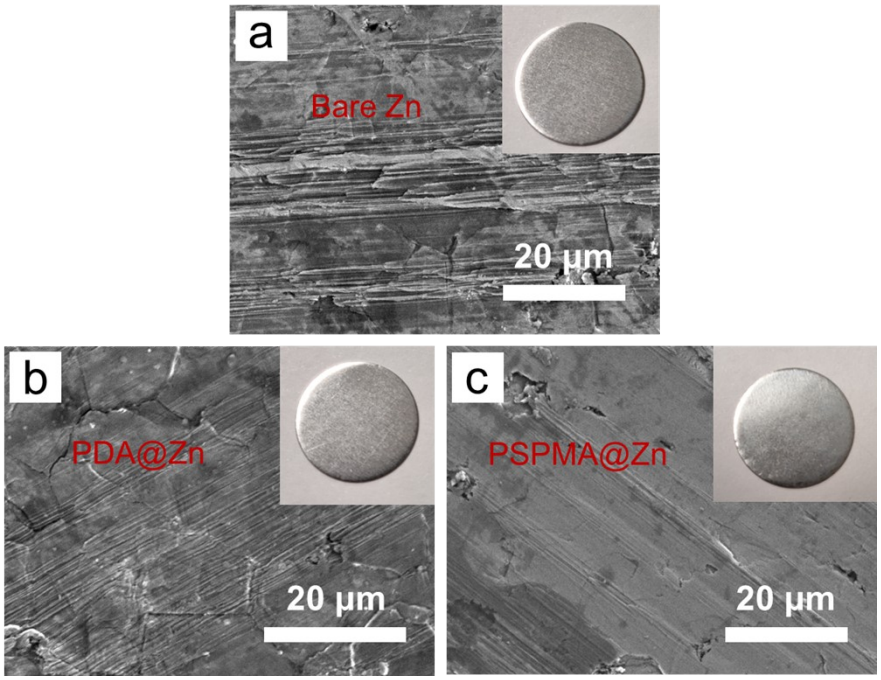

Fig. S1 The digital photographs and SEM images of (a) bare Zn, (b) PDA@Zn, and (c) PSPMA@Zn

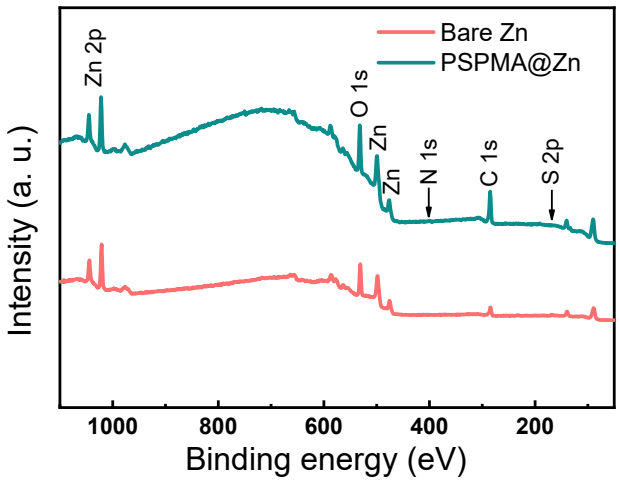

Fig. S2 The survey XPS spectra of bare Zn and PSPMA@Zn electrodes.

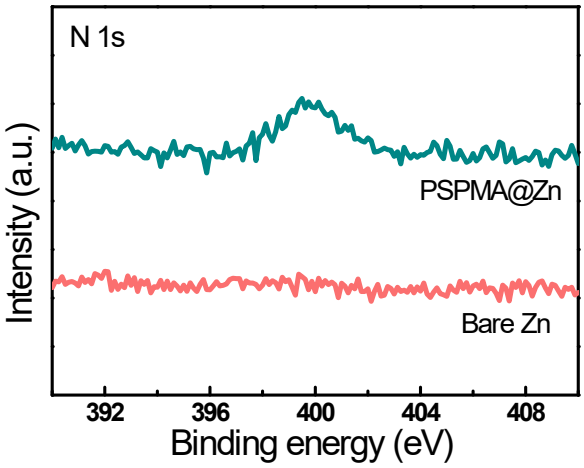

Fig. S3 High-resolution N 1s XPS spectra of bare Zn and PSPMA@Zn.

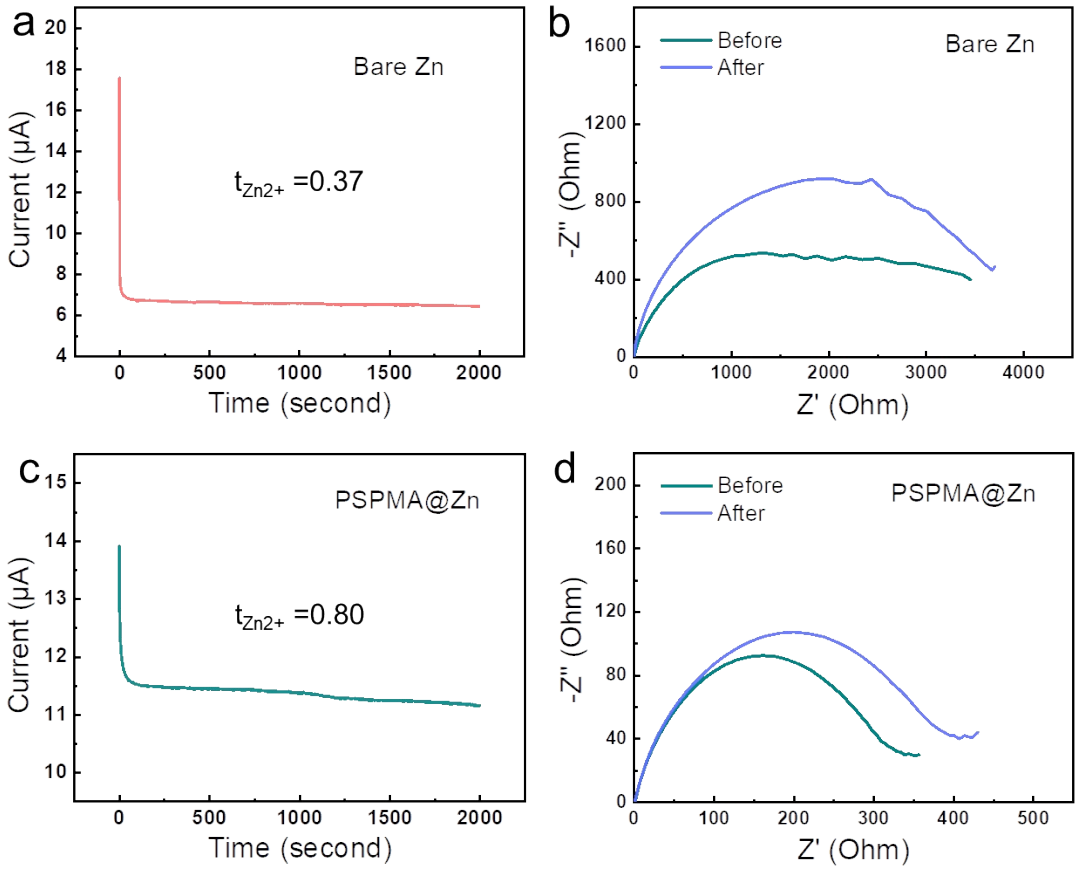

Fig. S4 Current variation with time during polarization and the associated EIS curves of (a, b) bare Zn and (c, d) PSPMA@Zn symmetrical cells with applied potential difference of 15 mV.

The Zn^{2+} transference number (t_{Zn2+}) was calculated according to the Bruce-Vincent method:

$$t_{Zn^{2+}} = \frac{I_s(V - I_0R_0)}{I_0(V - I_sR_s)} \quad (1)$$

Where V is the applied potential (15 mV); I_0 and R_0 are the initial current and interface resistance, respectively; I_s and R_s represent the steady-state current and interface resistance, respectively. Therefore, the $t_{Zn^{2+}}$ value in PSPMA@Zn system can be calculated to 0.80, whereas the value in bare Zn system is only 0.37.

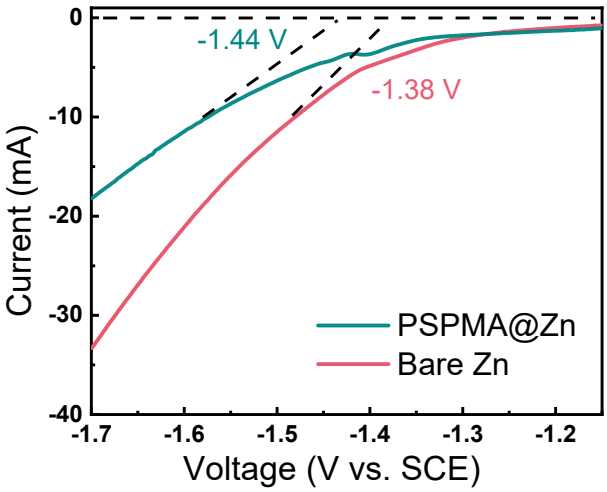

Fig. S5 LSV curves of bare Zn and PSPMA@Zn electrodes in 1 M Na_2SO_4 aqueous electrolyte.

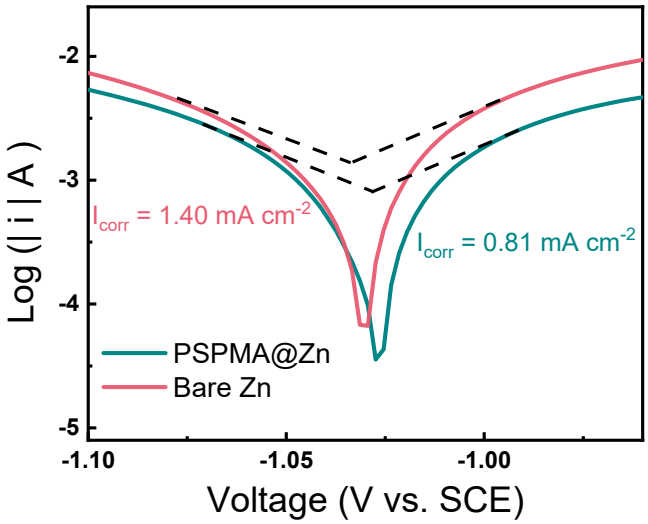

Fig. S6 Linear polarization curves of bare Zn and PSPMA@Zn electrodes.

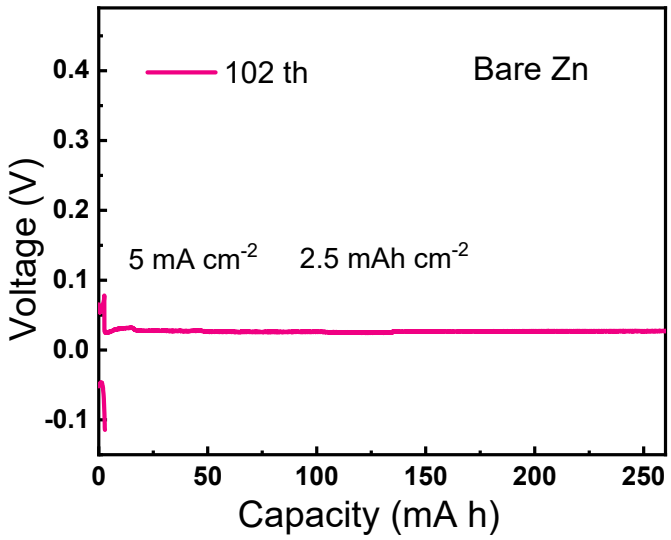

Fig. S7 The discharge-charge curve of bare Zn symmetric battery at 102 cycles, illustrating the battery short-circuit.

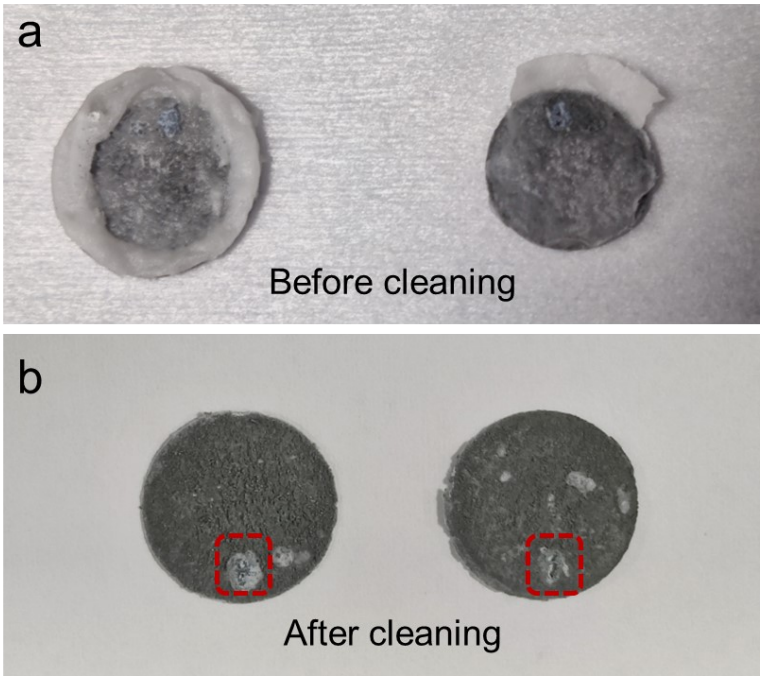

Fig. S8 The post-mortem optical images of the disassembled bare Zn (a) before cleaning and (b) after cleaning.

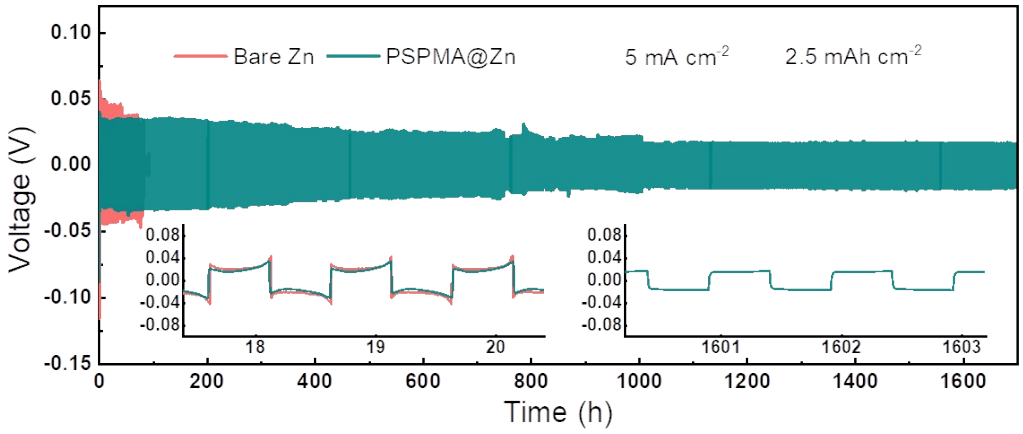

Fig. S9 Cycling performance of bare Zn and PSPMA@Zn symmetric cell at 5 mA cm^{-2} for 2.5 mAh cm^{-2}.

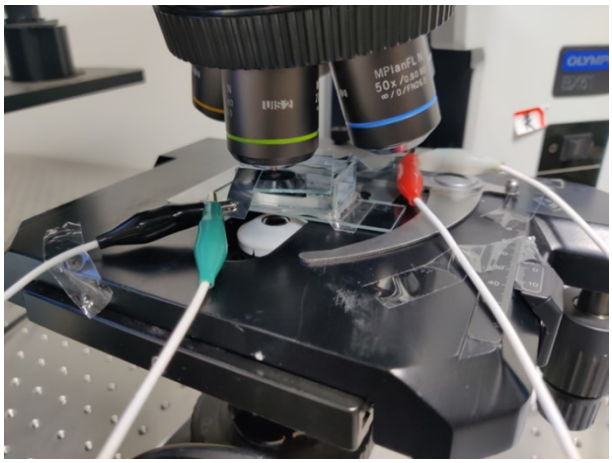

Fig. S10 Self-made symmetric cell model for in-situ optical microscope.

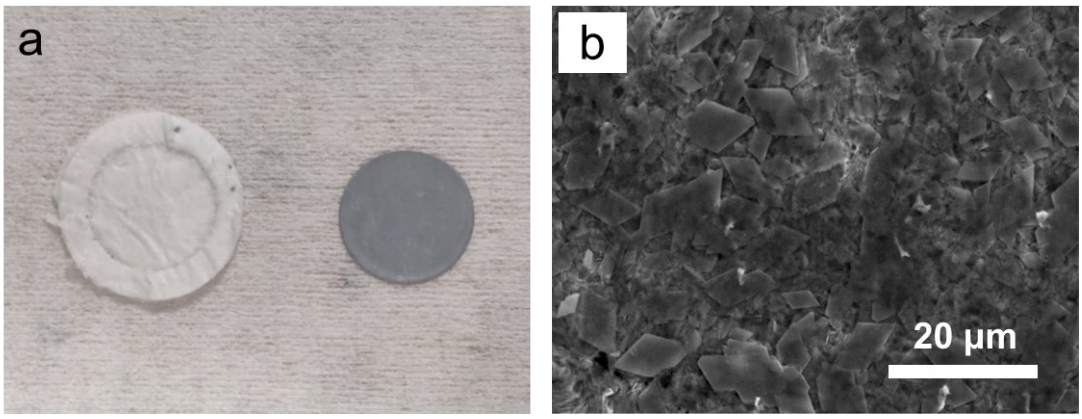

Fig. S11 (a) Detached PSPMA@Zn cell after 50 cycles at 1 mA cm^{-2} and 0.5 mAh cm^{-2}. (b) Top-view SEM image of PSPMA@Zn electrode.

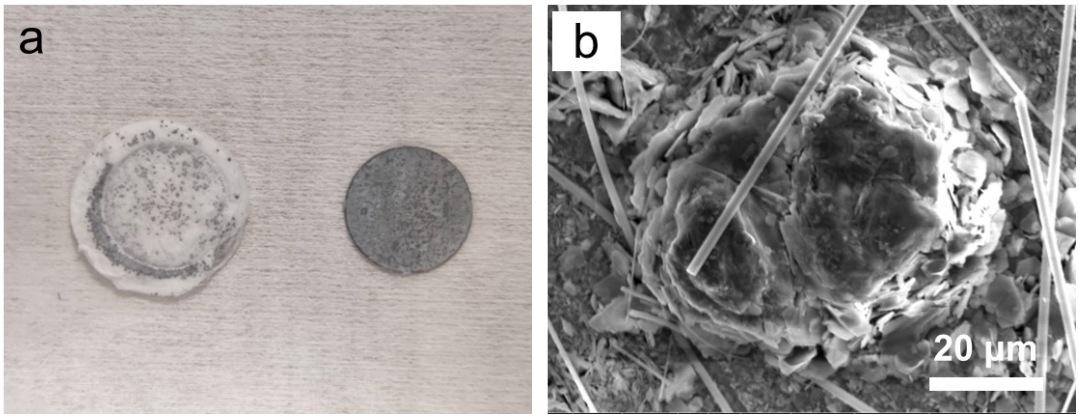

Fig. S12 (a) Detached bare Zn cell after 50 cycles at 1 mA cm^{-2} and 0.5 mAh cm^{-2}. (b) Top-view SEM image of bare Zn electrode.

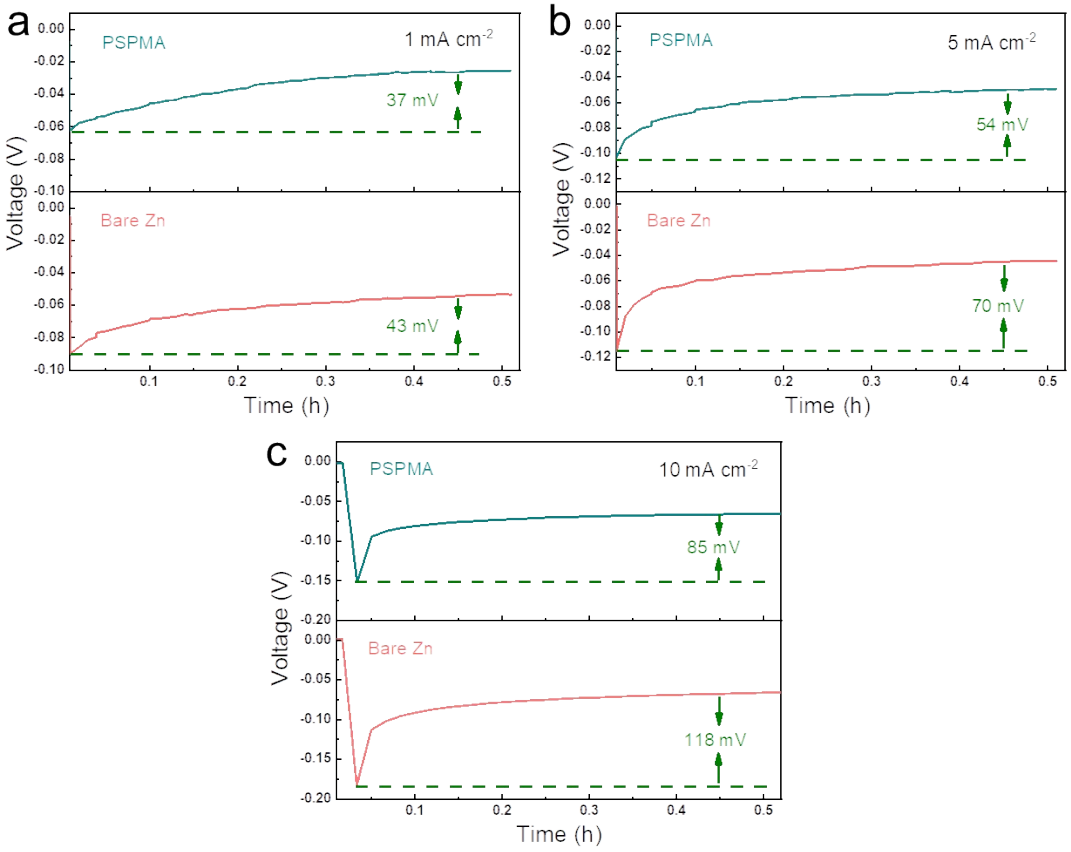

Fig. S13 Nucleation overpotential of bare Zn and PSPMA@Zn symmetric cells at (a) 1 mA cm^{-2}, (b) 5 mA cm^{-2}, and (c) 10 mA cm^{-2}.

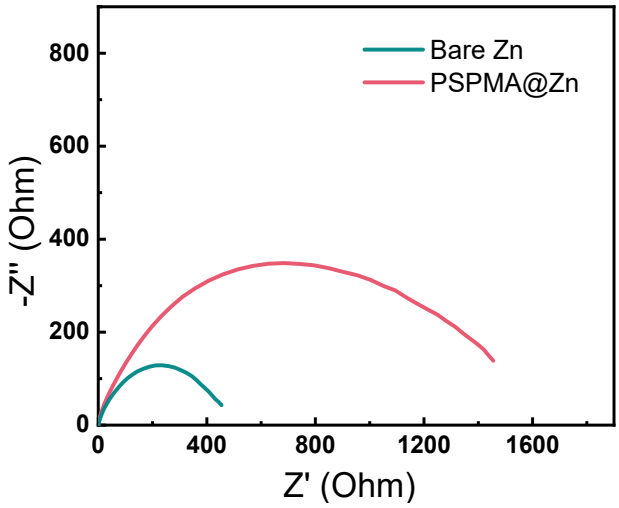

Fig. S14 Comparison of EIS curve of the PSPMA@Zn and bare Zn symmetric cells.

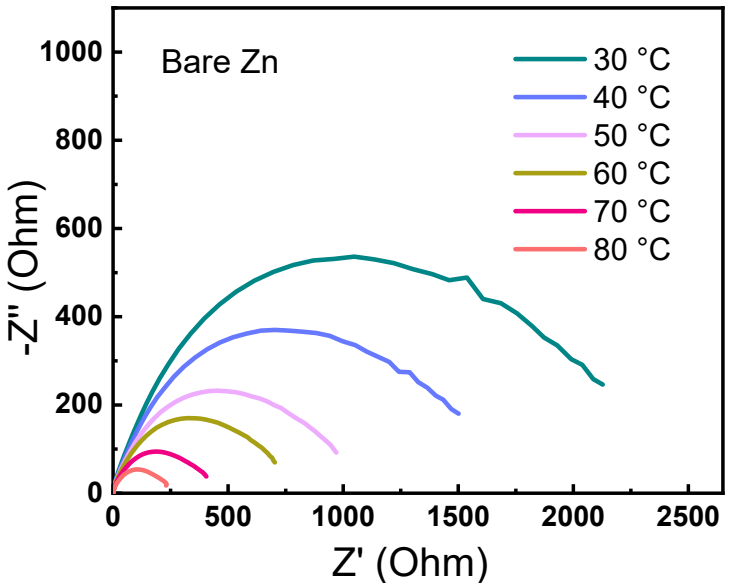

Fig. S15 EIS curves of bare Zn at different temperatures.

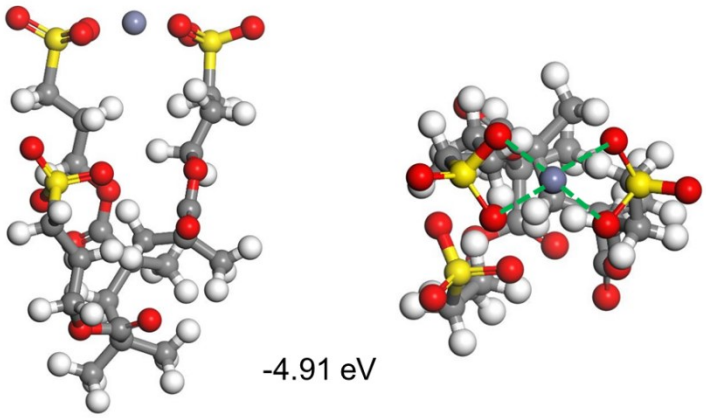

Fig. S16 Theoretical calcualtion model of Zn^{2+} in between the PSPMA molecular brushes.

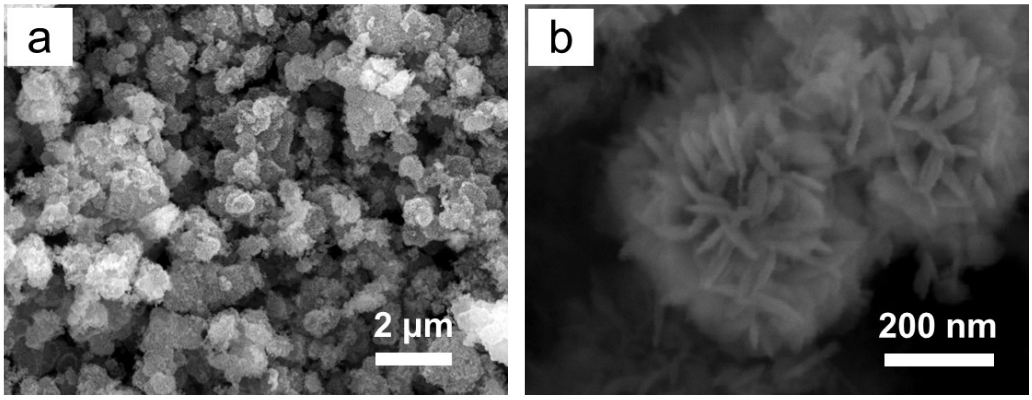

Fig. S17 SEM images of the prepared MnO_2 sample.

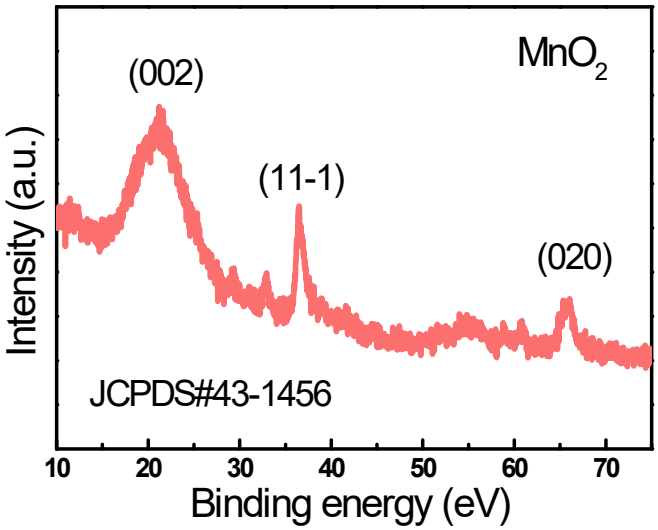

Fig. S18 XRD pattern of the prepared MnO_2 sample.

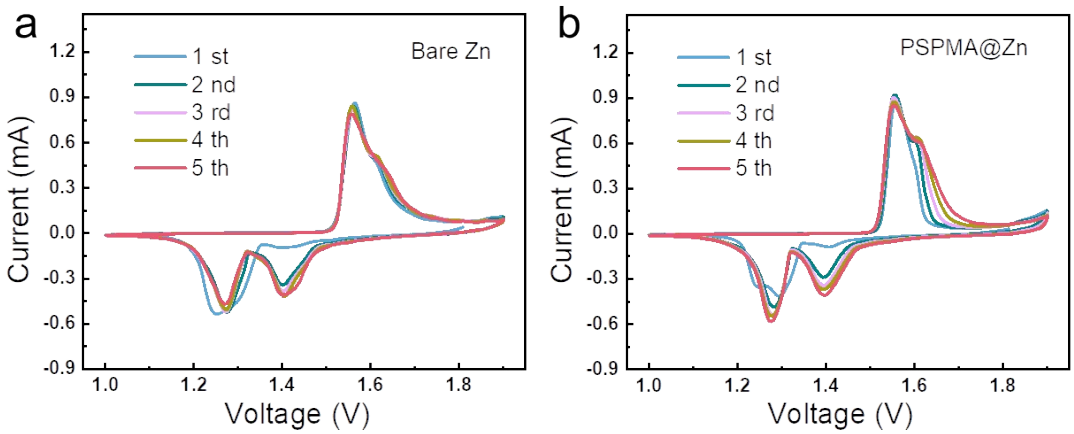

Fig. S19 CV curves of (a) bare Zn||MnO_2 and (b) PSPMA@Zn||MnO_2 cells at a scan rate of 0.1 mV s^{-1}.

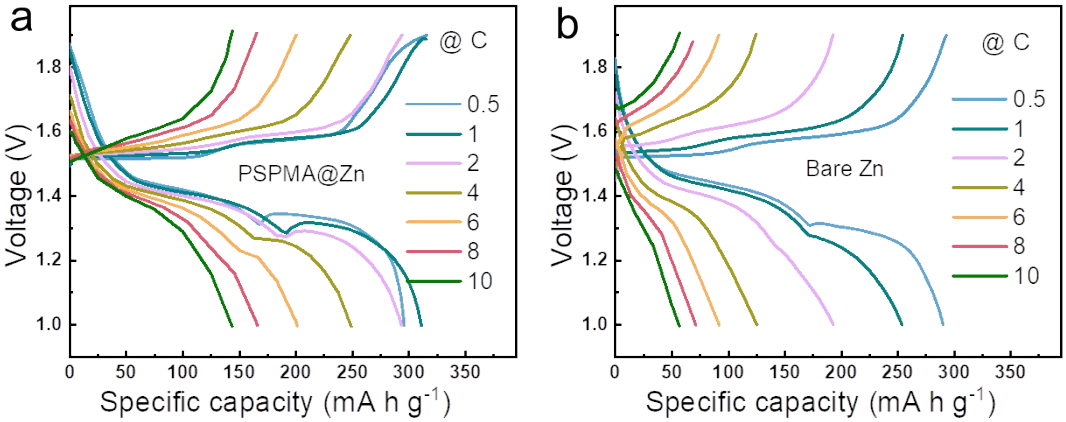

Fig. S20 Charge-discharge profiles of (a) PSPMA@Zn||MnO_2 and (b) bare Zn||MnO_2 cells at current densities from 0.5 C to 10 C. (1C = 308 mAh g^{-1})

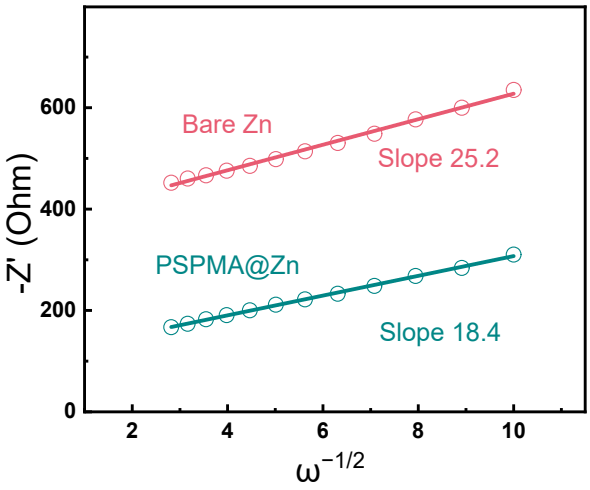

Fig. S21 Z'~$\omega^{-1/2}$ fitting curves of the full cells based on EIS results.

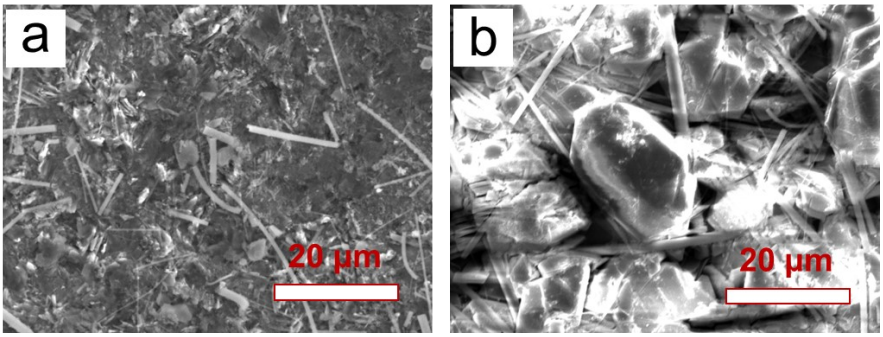

Fig. S22 SEM images of bare Zn and PSPMA@Zn electrodes in full cells after cycling.

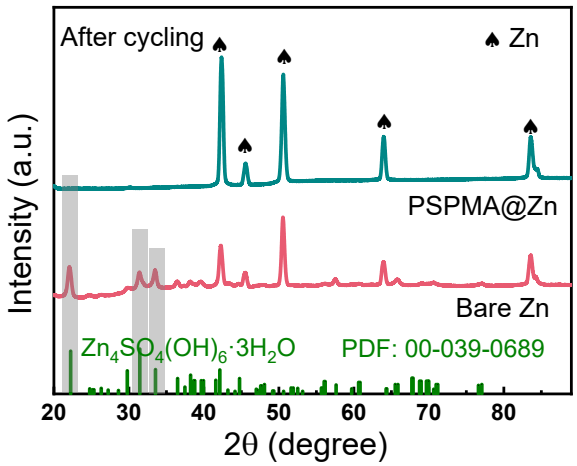

Fig. S23 XRD patterns of bare Zn and PSPMA@Zn electrodes in full cells after cycling.

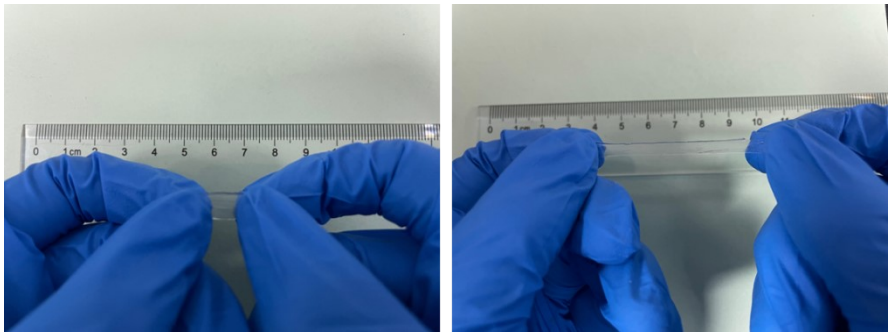

Fig. S24 The flexible PAM gel electrolyte that can be stretched to 600%.

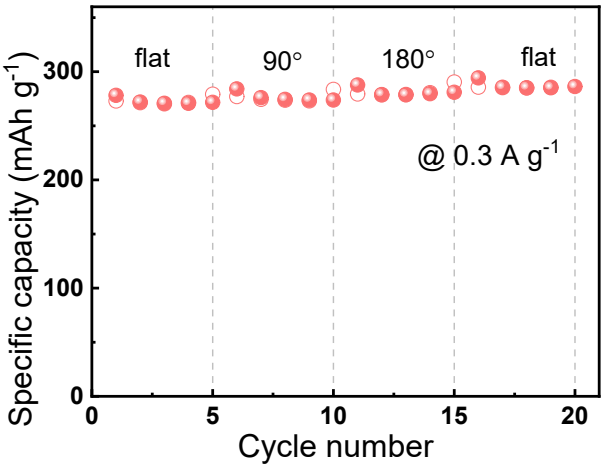

Fig. S25 The electrochemical performance of the flexible Zn-MnO_2 cell under different deformation degrees.

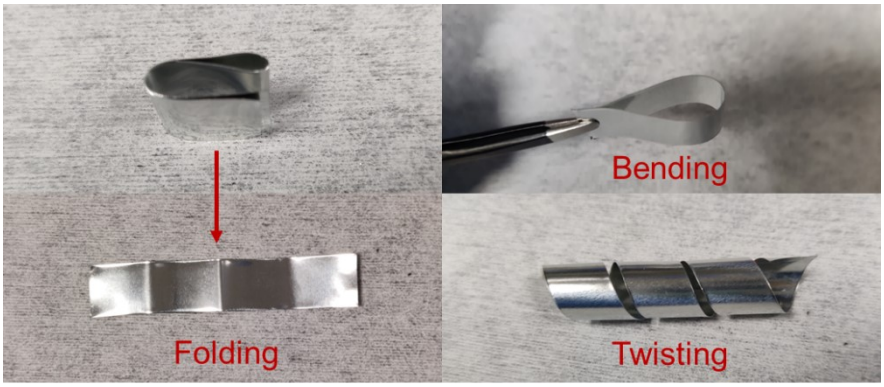

Fig. S26 Optical images of PDA-g-PSPMA@Zn anode under bending, folding, and twisting states.

Fig. S27 Digital graphs of the flexible cell powering an electronic watchband.

Table S1 The comparison of CPC and average CE with other reported artificial protective layers.

Coating layer	Current density (mA cm^{-2})	Average CE (%)	CPC (Ah cm^{-2})	Reference
PSPMA	5	99.9	2.25	This work
3D-ZnO	2	99.5	0.15	[1]
ZnS	2	99.2	0.2	[2]
CNG	0.5	99.4	0.15	[3]
PVB	4	99.4	0.2	[4]
MOF	0.5	99.9	0.175	[5]
COF	1	99.5	0.5	[6]
Zn-PA	2	99.9	0.8	[7]
Nafion-Zn-X	0.5	99.7	0.065	[8]

Table S2 The CPC comparison of PSPMA@Zn symmetric cell with other reported literature.

Coating layer	Current density (mA cm^{-2})	Areal capacity per cycle (mAh cm^{-2})	CPC (Ah cm^{-2})	Reference
PSPMA	10	5	12.5	This work
3D-ZnO	5	1.25	1.25	[1]
ZnS	2	2	1.1	[2]
TiO_2	2	2	0.28	[9]
Kaolin	4.4	1.1	1.76	[10]
$Zn_3(PO_4)_2$	5	1	0.55	[11]
CNG	1	0.5	1.5	[3]
CaF_2	4.4	1.1	2.2	[12]
COF	3	3	1.8	[6]
Polyamide	0.5	0.25	2	[13]
PVB	0.5	0.5	1.1	[4]
Zn-PA	5	2.5	4.25	[7]
Polyimide	4	2	1.7	[14]
Nafion-Zn-X	5	0.5	0.5	[8]

References

1. X. Xie, S. Liang, J. Gao, S. Guo, J. Guo, C. Wang, G. Xu, X. Wu, G. Chen and J. Zhou, *Energy Environ. Sci.*, 2020, **13**, 503-510.

2. J. Hao, B. Li, X. Li, X. Zeng, S. Zhang, F. Yang, S. Liu, D. Li, C. Wu and Z. Guo, *Adv. Mater.*, 2020, **32**, 2003021.

3. X. Zhang, J. Li, D. Liu, M. Liu, T. Zhou, K. Qi, L. Shi, Y. Zhu and Y. Qian, *Energy Environ. Sci.*, 2021, **14**, 3120-3129

4. J. Hao, X. Li, S. Zhang, F. Yang, X. Zeng, S. Zhang, G. Bo, C. Wang and Z. Guo, *Adv. Funct. Mater.*, 2020, **30**, 2001263.

5. L. Cao, D. Li, T. Deng, Q. Li and C. Wang, *Angew. Chem. Int. Ed.*, 2020, **59**, 19292-19296.

6. K. Wu, X. Shi, F. Yu, H. Liu, Y. Zhang, M. Wu, H.-K. Liu, S.-X. Dou, Y. Wang and C. Wu, *Energy Storage Mater.*, 2022, **51**, 391-399.

7. H. Liu, J. Wang, W. Hua, L. Ren, H. Sun, Z. Hou, Y. Huyan, Y. Cao, C. Wei and F. Kang, *Energy Environ. Sci.*, 2022, **15**, 1872-1881.

8. Y. Cui, Q. Zhao, X. Wu, X. Chen, J. Yang, Y. Wang, R. Qin, S. Ding, Y. Song, J. Wu, K. Yang, Z. Wang, Z. Mei, Z. Song, H. Wu, Z. Jiang, G. Qian, L. Yang and F. Pan, *Angew. Chem. Int. Ed.*, 2020, **132**, 16737-16744.

9. Q. Zhang, J. Luan, X. Huang, Q. Wang, D. Sun, Y. Tang, X. Ji and H. Wang, *Nat. Commun.*, 2020, **11**, 3961.

10. C. Deng, X. Xie, J. Han, Y. Tang, J. Gao, C. Liu, X. Shi, J. Zhou and S. Liang, *Adv. Funct. Mater.*, 2020, **30**, 2000599.

11. X. Zeng, J. Mao, J. Hao, J. Liu, S. Liu, Z. Wang, Y. Wang, S. Zhang, T. Zheng, J. Liu, P. Rao and Z. Guo, *Adv. Mater.*, 2021, **33**, 2007416.

12. Y. Li, S. Yang, H. Du, Y. Liu, X. Wu, C. Yin, D. Wang, X. Wu, Z. He and X. Wu, *J. Mater. Chem. A*, 2022, **10**, 14399-14410.

13. Z. Zhao, J. Zhao, Z. Hu, J. Li, J. Li, Y. Zhang, C. Wang and G. Cui, *Energy Environ. Sci.*, 2019, **12**, 1938-1949.

14. M. Zhu, J. Hu, Q. Lu, H. Dong, D. D. Karnaushenko, C. Becker, D. Karnaushenko, Y. Li, H. Tang, Z. Qu, J. Ge and O. G. Schmidt, *Adv. Mater.*, 2021, **33**, 2007497.